JACS
JOURNAL OF THE AMERICAN CHEMICAL SOCIETY

ARTICLE

pubs.acs.org/JACS

Single-Molecule Force Spectroscopy of β-Peptides That Display Well-Defined Three-Dimensional Chemical Patterns

Claribel Acevedo-Vélez,[†] Guillaume Andre,[§] Yves F. Dufrêne,[§] Samuel H. Gellman,[‡] and Nicholas L. Abbott*[,†]

[†]Department of Chemical and Biological Engineering, University of Wisconsin—Madison, 1415 Engineering Drive, Madison, Wisconsin 53706, United States

[‡]Department of Chemistry, University of Wisconsin—Madison, 1101 University Avenue, Madison, Wisconsin 53706, United States

[§]Institute of Condensed Matter and Nanosciences-Bio & Soft Matter, Université Catholique de Louvain, Croix du Sud 2/18, B-1348 Louvain-la-Neuve, Belgium

Supporting Information

ABSTRACT: Oligomers of β-amino acids ("β-peptides") can be designed to fold into *stable* helices that display side chains with a diverse range of chemical functionality in precise arrangements. We sought to determine whether the predictable, three-dimensional side-chain patterns generated by β-peptides could be used in combination with single-molecule force spectroscopy to quantify how changes in nanometer-scale chemical patterns affect intermolecular interactions. To this end, we synthesized β-peptides that were designed to be either globally amphiphilic (**GA**), i.e., display a global segregation of side chains bearing hydrophobic and cationic functional groups, or non-globally amphiphilic (***iso*-GA**), i.e., display a more uniform distribution of hydrophobic and cationic functional groups in three-dimensions. Single-molecule force measurements of β-peptide interactions with hydrophobic surfaces through aqueous solution (triethanolamine buffer, pH 7.2) reveal that the **GA** and ***iso*-GA** isomers give rise to qualitatively different adhesion force histograms. The data are consistent with the display of a substantial nonpolar domain by the **GA** oligomer, which leads to strong hydrophobic interactions, and the absence of a comparable domain on the ***iso*-GA** oligomer. This interpretation is supported by force measurements in the presence of methanol, which is known to disrupt hydrophobic interactions. Our ability to associate changes in measured forces with changes in three-dimensional chemical nanopatterns projected from conformationally stable β-peptide helices highlights a contrast between this system and conventional peptides (α-amino acid residues): conventional peptides are more conformationally flexible, which leads to uncertainty in the three-dimensional nanoscopic chemical patterns that underlie measured forces. Overall, we conclude that β-peptide oligomers provide a versatile platform for quantifying intermolecular interactions that arise from specific functional group nanopatterns.

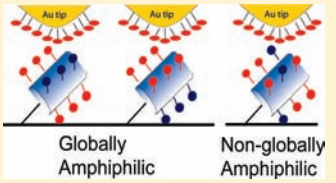

INTRODUCTION

The rational design of self-assembled materials requires an understanding of how intermolecular interactions are directed by the three-dimensional patterns in which functional groups are displayed from a molecular backbone.[1] For some molecular systems, such as those interacting through nucleotide base pairing, remarkably complex structures (e.g., DNA origami) can be designed simply through specification of the subunit sequence.[2−4] For many other molecular systems, including those that associate through "hydrophobic" interactions (as measured, for example, using the surface force apparatus and the atomic force microscope),[5−12] an understanding of how patterns of nonpolar, uncharged polar, and ionic functional groups combine to direct intermolecular associations in aqueous solution remains to be fully developed. A number of theoretical studies, simulations, and experimental observations support the view that hydrophobic interactions mediated by water are size dependent, with a crossover in thermodynamic profile occurring for hydrophobic domains with sizes around 1 nm^2.[10−12] For example, at low temperatures, it has been noted that the entropy of hydrating small hydrophobic molecules (<1 nm^2, e.g., alkanes) is negative, whereas for extended hydrophobic surfaces (>1 nm^2) the entropy of hydration is positive.[10] The potential existence of such a discontinuity raises many questions that remain unexplored, such as the thermodynamics of interactions involving hydrophobic domains with irregular shapes, the effect of introducing one isolated hydrophilic group (or more) into a hydrophobic domain, and the impact of the complex topographies commonly observed at biomacromolecular interfaces on the energetics of interactions involving those interfaces.[12]

As a step toward establishing a methodology to elucidate the intermolecular forces generated by complex patterns of chemical functionality, we report here the use of single-molecule force spectroscopy[13] to characterize the intermolecular interactions of β-amino acid oligomers ("β-peptides";[14−16] Figure 1). As detailed below, β-peptides are unusual in enabling the design of very stable helical secondary structures that present predictable

Received: October 3, 2010
Published: March 01, 2011

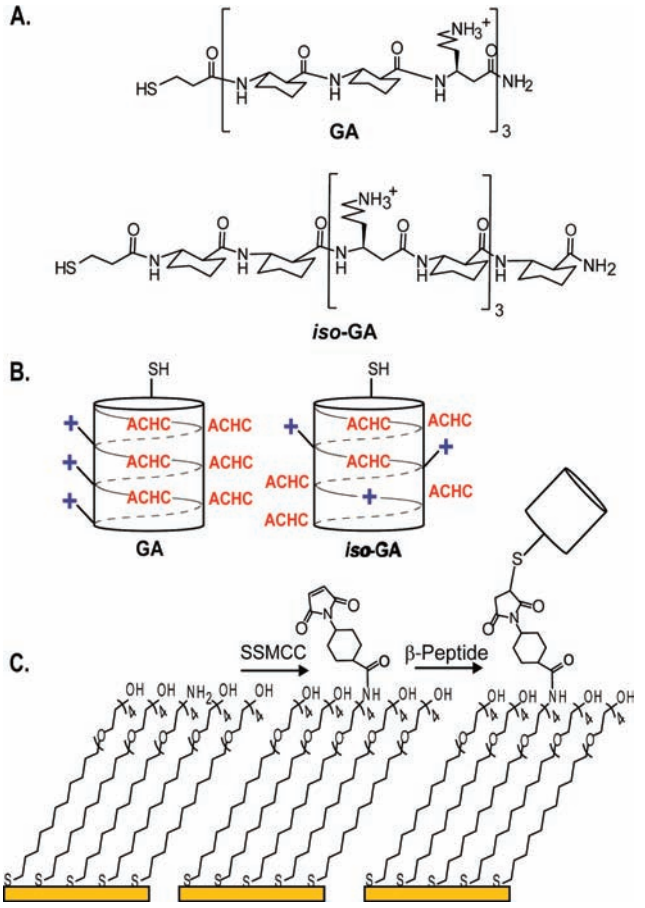

Figure 1. (A) Globally amphiphilic (**GA**) and nonglobally amphiphilic (***iso*-GA**) β-peptide sequence isomers used in this study. (B) Schematic representation of the isomers with rigid helical conformations. (C) Chemistry used to immobilize β-peptide oligomers for single-molecule force measurements.

and precisely defined nanoscopic patterns of chemical functionality in three dimensions. Our results suggest that β-peptide oligomers, when combined with single-molecule force spectroscopy, form the basis of a general and facile approach to exploring how chemical nanopatterns define intermolecular interactions.

Single-molecule force spectroscopy measurements have been reported for a variety of peptides and proteins (α-amino acid subunits). For example, structural and conformational changes and cis−trans isomerization in proteins induced by external forces[17−19] or by the binding of a ligand,[20] changes in polypeptide molecular elasticity,[21] and changes in intermolecular interactions between proteins[22] in response to environmental stimuli have been investigated. In addition, several investigators have examined specific interactions involving other types of biomolecules including (i) the interactions between antibiotics and bacterial cells,[23] (ii) antigen−antibody[24−26] and receptor−ligand interactions,[27−29] (iii) protein-mediated cell adhesion,[30] or (iv) interactions between complementary strands of DNA.[31] Of particular relevance to this paper are studies of hydrophobic interactions using single-molecule force spectroscopy.[32−35] For example, single-molecule force spectroscopy measurements of hydrophobic interactions between molecules with relatively simple structures, such as tethered linear alkanes, have been reported.[32] In addition, single-molecule interactions between α-peptides and hydrophobic surfaces have been investigated in an effort to provide insights into the mechanisms governing polypeptide adsorption at hydrophobic interfaces,[34] protein folding, and self-assembly in aqueous environments.[35] While these latter studies have permitted quantification of forces, the complexity of the structures of full-fledged proteins and the lack of stable secondary structure in oligo-α-peptides (including the tendency of the secondary structure to change in response to environmental variations) prevent identification of the exact three-dimensional nanoscopic chemical patterns that are responsible for the measured forces in these cases.

The study reported here goes beyond these precedents because our force measurements involve β-peptides, which can be designed to adopt helical conformations with much greater stability than can be achieved among conventional α-peptides. Because the β-peptide helices have been characterized at atomic resolution, it is possible to design β-amino acid sequences that give rise to specific three-dimensional patterns of side chains that bear a variety of functional groups.[36−40] The experiments described below are based on the 14-helix, which is defined by 14-membered ring C=O(i)···H−N(i-2) H bonds between backbone amides and contains approximately three residues per helical turn. β-Peptides that adopt 14-helical secondary structure have been extensively studied.[41−46] Incorporation of cyclically constrained *trans*-2-aminocyclohexanecarboxylic acid (ACHC) residues confers very high 14-helical stability. Short ACHC-rich β-peptides display a much higher helix stability than can be achieved with conventional α-peptides of comparable length.[37−40] 14-Helical β-peptides containing ≥50% ACHC residues appear to be more or less fully folded in aqueous solution. The high stability of the 14-helix and the ability to specify the β-amino acid sequence via synthesis allow very precise control of the nanoscale patterning of chemical functional groups on the surfaces of these oligomers.

A number of past studies have reported on the self-assembly of β-peptides that favor 14-helical secondary structure.[41−45] These studies reveal that subtle variations in the nanopatterning of chemical functional groups on the surface of the 14-helix, as can occur between sequence isomers, exert dramatic effects on self-assembly behavior. For example, sequence-dependence has been observed in self-assembly of catalytically active nanoclusters[45] and formation of hollow nanotubes[42,43] and liquid crystalline phases[41,42] have been observed. On the basis of these precedents in bulk solution, we sought to determine whether single-molecule force spectroscopy could be used to measure differences in the intermolecular forces generated by surface-immobilized β-peptide sequence isomers that present distinct three-dimensional chemical nanopatterns. Below we report measurements of interactions involving isomeric β-peptide oligomers that contain hydrophobic (ACHC) and cationic (β^3-homolysine (β^3-hLys)) side chains (Figure 1A). For the globally amphiphilic isomer (**GA**), the ACHC and β^3-hLys residues segregate to opposite sides of the 14-helix, but such segregation is *not* achieved in the 14-helical conformation of the non-globally amphiphilic sequence isomer (***iso*-GA**) (Figure 1B).

EXPERIMENTAL SECTION

Materials. The 14-helical β-peptides used in this study were synthesized by solid-phase methods as described elsewhere.[46] Tetraethylene glycol thiols terminated in hydroxyl (EG4) or amine groups (EG4N) were purchased from Prochimia (Poland). 1-Dodecanethiol

dx.doi.org/10.1021/ja1089183 |*J. Am. Chem. Soc.* 2011, 133, 3981–3988

(98%), β-mercaptoethanol (98%), triethanolamine (TEA) HCl (99%), and methanol (anhydrous, 99.8%) were purchased from Aldrich (Milwaukee, WI). Sulfosuccinimidyl-4-(*N*-maleimidomethyl)cyclohexane-1-carboxylate (SSMCC) was purchased from Pierce Biotechnology (Rockford, IL). Ethanol (reagent, anhydrous, denatured) used for preparation of thiol solutions and sodium chloride (99.0%) were purchased from Sigma-Aldrich (Milwaukee, WI). Ethanol (anhydrous, 200 proof) used for rinsing was purchased from Pharmco-AAPER (Shelbyville, MA). Deionized water used in the study had a resistivity of 18.2 MΩ-cm. All chemicals were used as received and without any further purification. The AFM tips used in this study (triangular shaped, nominal spring constant of 0.01 N/m, and radius of curvature of 10 nm) were purchased from Veeco Metrology (Santa Barbara, CA). Silicon wafers were purchased from Silicon Sense (Nashua, NH).

Gold Deposition on Silicon Substrates and AFM Tips. AFM tips and silicon wafers were coated with a 5 nm layer of titanium and a 30 nm layer of gold at normal incidence using an electron beam evaporator (Tek-Vac Industries, Brentwood, NY). The rates of deposition of gold and titanium were ∼0.2 Å/s. The pressure in the evaporator was maintained at less than 1×10^{-6} Torr throughout evaporation of the metals. Gold-coated substrates and tips were used immediately after gold deposition.

Preparation of Chemically Functionalized AFM Tips. Following gold deposition, the AFM tips were immersed in a 1 mM ethanolic solution of 1-dodecanethiol and incubated overnight. Upon removal from solution, the tips were rinsed with ethanol, dried with a gentle stream of nitrogen, and immediately transferred to the AFM fluid cell.

Preparation of β-Peptide-Decorated Surfaces. Following gold deposition, the silicon wafers were cut into small pieces, immersed in an ethanolic solution composed of 2 μM EG4N and 0.998 mM EG4, and incubated for 18 h. The substrates were then rinsed with ethanol and deionized water (3× each) and dried with a stream of nitrogen. Subsequently, the surfaces were treated with the SSMCC cross-linker (1 mg/mL solution in TEA buffer, pH 7.2) for 1 h, rinsed with deionized water and ethanol, and dried with nitrogen. Finally, the maleimide-activated surfaces were reacted with the thiol-terminated β-peptides (250 μM solution in TEA buffer, pH 7.2) for 3 h. The surfaces were then rinsed thoroughly using the following procedure: 100 mM TEA buffer (pH 7.2), deionized water, 100 mM NaCl, deionized water, methanol, deionized water. The surfaces were then dried with nitrogen and stored in TEA buffer (pH 7.2) until AFM force measurements were performed.

Characterization of β-Peptide-Decorated Surfaces. Prior to performing AFM force measurements, we characterized these surfaces by ellipsometry, X-ray photoelectron spectroscopy, and AFM imaging. Ellipsometry was used to characterize the increment in optical thicknesses of the surfaces at the different steps of the immobilization procedure. Ellipsometric measurements were performed with a Gaertner LSE ellipsometer ($\lambda = 632.8$ nm, $\psi = 70°$). The optical thicknesses reported in Table 1 are the averages of three independent experiments (with three replicates each) using a refractive index of $n = 1.46$ for the thin films.

X-ray photoelectron spectroscopy (XPS) was used to determine the atomic composition of the surfaces at the various steps of the immobilization procedure, as reported in Table 1. The major peaks of interest were N (1s), C (1s), O (1s), and Au (4f). The Perkin-Elmer PHI 5400 XPS system was equipped with Omni-Focus Lens and a magnesium X-ray source (1486.6 eV). The XPS spectra were obtained over an approximate surface area of 1 mm × 3 mm. Survey scans with a pass energy of 89.45 eV were first performed to identify elements present on the surface, followed by acquisition of element-specific spectra with a pass energy of 0.5 eV. Data analysis was performed using the RBD Instruments AugerScan analysis software. The atomic composition of each element present on the surface was determined, after establishing the baselines, by integrating the area under each peak and correcting for the element-specific PHI sensitivity factors. The atomic compositions reported in Table 1 are the average of two independent experiments.

AFM imaging was performed in order to verify that the surfaces were homogeneous and free of aggregates (See Supporting Information, Figure S1). AFM images were obtained using a Nanoscope IIIa Multimode AFM equipped with a fluid cell (Veeco Metrology Group, Santa Barbara, CA) in deionized water using contact mode and triangular-shaped silicon nitride cantilevers (nominal spring constant of 0.01 N/m and radius of curvature of 10 nm).

AFM Force Measurements. Adhesion force measurements were performed using a Nanoscope IIIa Multimode AFM equipped with a fluid cell (Veeco Metrology Group, Santa Barbara, CA). Force measurements were performed at room temperature. Contact-time was kept constant at 0 ms. Retraction and approach speed were kept constant at 1000 nm/s. Triangular-shaped silicon nitride cantilevers were used and functionalized as described above. The spring constants of the cantilevers were calibrated using Sader's method on a PCM-90 Spring Constant Calibration Module (Novascan Technologies, Aimes, IA) and determined to be ∼0.011 N/m. Force curves were recorded by moving the AFM tip over different places on the sample, and at least 100 force curves were recorded at each spot in order to plot adhesion force histograms. All forces were recorded with a constant contact force of ∼0.2 nN to avoid tip and surface damage.

RESULTS

We measured the interactions of surface-immobilized β-peptides with the tip of an atomic force microscope (AFM) that was coated with gold and subsequently modified chemically to be hydrophobic[47,48] by reaction with 1-dodecanethiol. To perform these measurements, we covalently immobilized the β-peptides at surfaces such that (1) the β-peptides were presented at a sufficiently low density to enable measurement of single-molecule interactions with the AFM tip (see below for additional discussion) and (2) no adhesive interactions occurred between the hydrophobic AFM tip and the surface in the absence of β-peptide. These goals were achieved as shown in Figure 1C. We prepared mixed self-assembled monolayers on gold substrates from thiols containing tetraethylene glycol that were terminated with either hydroxyl (EG4) or primary amine (EG4N). The amine groups of EG4N were acylated with the cross-linker sulfosuccinimidyl-4-(*N*-maleimidomethyl)cyclohexane-1-carboxylate (SSMCC), and the maleimide unit of SSMCC was then used to covalently attach the thiol-terminated β-peptides to the monolayers.[49] This chemistry has been widely used in past studies in which oligopeptides have been immobilized on surfaces at controlled densities.[50] A low density of surface-immobilized β-peptide was achieved by preparing mixed monolayers containing 0.2% EG4N.

We used a combination of X-ray photoelectron spectroscopy (XPS) and ellipsometry to confirm immobilization of the β-peptides on the surfaces (Table 1). The increment in optical thickness (∼1 nm) measured after β-peptide immobilization on 100% EG4N surfaces is consistent with monolayer coverage of the β-peptide. Elemental analysis by XPS reported in Table 1 confirms the attachment of β-peptides to the surface. In particular, the gold signal was lower after immobilization of either β-peptide (3.2 ± 0.4%) than before immobilization (7.7 ± 1.1%); we attribute the attenuation of the gold signal to the presence of a β-peptide monolayer. In addition, the nitrogen signal on the surface increased after immobilization of either β-peptide, from 3.8 ± 1.0% to ∼7%, which is consistent with the presence of

Table 1. Ellipsometric Thickness (nm) and Elemental Analysis by XPS (atomic compositions shown as percentages) of Surfaces Prepared during Immobilization of β-Peptide Oligomers

	ellipsometric thickness (nm)		atomic composition (%)			
sample	total thickness	increment in thickness	Au	C	O	N
EG4N	3.1 ± 0.1		7.7 ± 1.1	64.0 ± 1.1	24.5 ± 1.3	3.8 ± 1.0
EG4N + SSMCC	4.5 ± 0.1	1.3 ± 0.1	4.5 ± 1.7	67.7 ± 1.8	22.2 ± 2.0	5.6 ± 0.5
EG4N + SSMCC + **GA**	5.4 ± 0.2	0.9 ± 0.3	3.2 ± 0.4	70.6 ± 0.7	18.9 ± 1.3	7.3 ± 0.1
EG4N + SSMCC + ***iso*-GA**	5.3 ± 0.2	0.8 ± 0.3	3.1 ± 0.1	67.8 ± 0.6	23.1 ± 1.1	6.7 ± 0.4

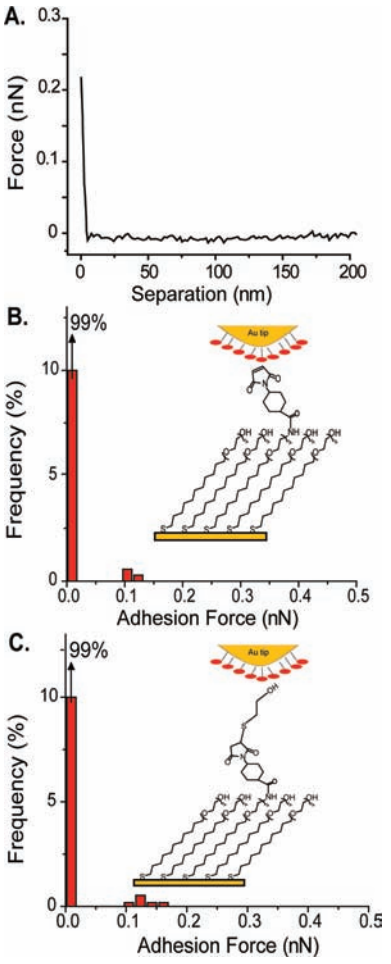

Figure 2. Force histograms and representative force−separation curves obtained using a hydrophobic AFM tip in TEA buffer (pH 7.2) for control force measurements. (A) Representative example of the force−separation curves obtained from control force measurements. (B) Force histogram for a maleimide-decorated surface prepared using SSMCC (as shown in Figure 1C). Inset shows a schematic illustration of the interaction between the maleimide group and the hydrophobic AFM tip (see text for details). (C) Force histogram after treatment of the surface in A with β-mercaptoethanol and then **GA** (see text for details). Inset shows a schematic illustration of the interaction between the β-mercaptoethanol and the hydrophobic AFM tip.

β-peptides on the surface. Although the atomic compositions of the β-peptide sequence isomers are identical, the carbon, oxygen, and nitrogen signals were not identical for the **GA** and ***iso*-GA** samples. The sources of these small differences in signal are unknown, but they may include factors such as the presence of residual waters of hydration as well as the attenuation of signals from buried functional groups. Prior to performing single-molecule force measurements, we characterized the β-peptide-decorated surfaces using AFM imaging, which confirmed that the surfaces were homogeneous and free of aggregates (Figure S1, Supporting Information).

Force measurement control studies were performed between the hydrophobic AFM tip and the surfaces at the different stages of the β-peptide immobilization procedure, namely, a pure monolayer of EG4, a mixed monolayer composed of 0.2% EG4N and 99.8% EG4, and a maleimide-decorated surface (0.2% EG4N after reaction with SSMCC). The measurements were performed in aqueous 100 mM triethanolamine (TEA) buffer at pH 7.2 (see Figure 2 and Supporting Information). The EG4N and maleimide groups should not be present on the surfaces presenting β-peptides if acylation and immobilization reactions go to completion; nevertheless, in control studies, we verified that these groups, if present, do not contribute significantly to measured adhesion forces (Figure 2B for a surface containing 0.2% EG4N; see also Supporting Information). No adhesion was detected for the surface bearing 0.2% SSMCC-activated EG4N; in contrast, significant adhesive forces were measured following incubation of either of the β-peptide sequence isomers, **GA** or ***iso*-GA**, with the SSMCC-activated surface (Figure 3C and Figure 3D, respectively). To establish that these forces result from β-peptides *covalently* immobilized, we measured adhesion forces using a SSMCC-activated monolayer that was pretreated with β-mercaptoethanol before incubation with thiol-terminated β-peptide (Figure 2C). The thiol group of β-mercaptoethanol should react with the maleimide groups of the SSMCC units, thus preventing covalent attachment of the β-peptides after pretreatment. Pretreatment with β-mercaptoethanol eliminated the adhesive interactions shown in Figure 3C and 3D, which leads us to conclude that the forces recorded in Figure 3C and 3D result from the interactions of covalently immobilized β-peptides and the hydrophobic AFM tip.

We conclude that the adhesion force histograms in Figure 3 correspond to single-molecule events for the following reasons. First, we considered it possible that the force histograms in Figure 3C and 3D (particularly, the strong adhesive interactions measured in the force histograms of the **GA** oligomers shown in Figure 3C) might correspond to the simultaneous interaction of two or more β-peptides with the AFM tip. To address this possibility, we monitored the fraction of nonadhesive interactions in our experiments and measured the force histograms on surfaces that generated a larger fraction of nonadhesive interactions. Inspection of Figure 3E and Figure 3F reveals that the force histograms obtained on surfaces with >90% nonadhesive interactions are similar to those shown in Figure 3C and 3D. The only

dx.doi.org/10.1021/ja1089183 |*J. Am. Chem. Soc.* 2011, 133, 3981–3988

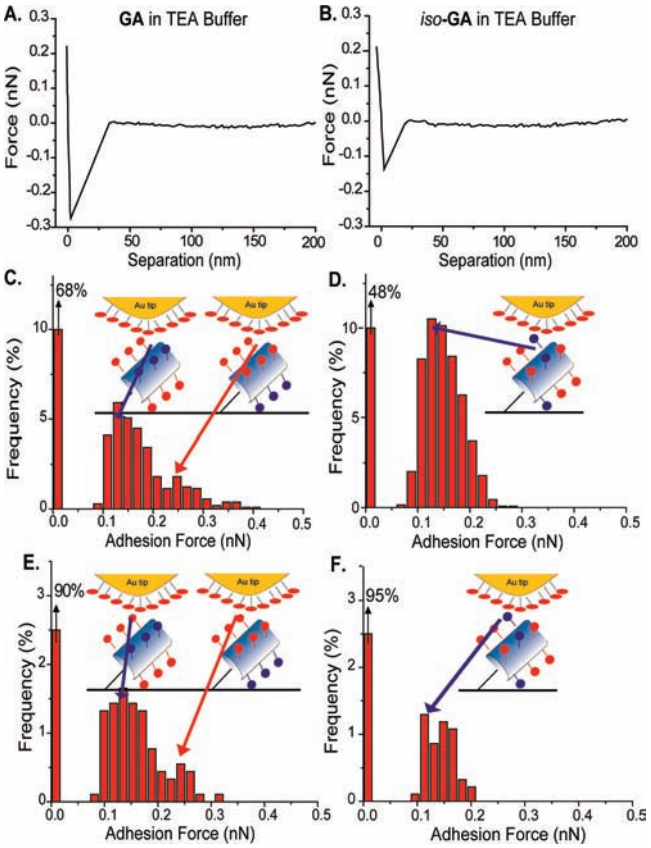

Figure 3. Force histograms and representative force−separation curves obtained between a hydrophobic AFM tip and a β-peptide-decorated surface in TEA buffer (pH 7.2). (A) Representative force−separation curve obtained for the surface in Figure 2B treated with **GA**. (B) Representative force−separation curve obtained for the surface in Figure 2B treated with ***iso*-GA**. (C) Force histograms for the surface in Figure 2B treated with **GA**. Inset shows a schematic illustration of the proposed interaction between a single **GA** β-peptide oligomer and a hydrophobic AFM tip (see text for details). The red and blue circles represent the hydrophobic ACHC groups and the cationic β^3-hLys groups around the β-peptide oligomer, respectively. (D) Force histogram for the surface in Figure 2B treated with ***iso*-GA**. Inset shows a schematic illustration of the proposed interaction between a single ***iso*-GA** β-peptide oligomer and a hydrophobic AFM tip (see text for details). (E) Force histograms for a surface presenting **GA** that led to ~90% nonadhesive contacts. (F) Force histogram for a surface presenting ***iso*-GA** that led to ~95% nonadhesive contacts. Force measurements were performed at constant approach and retraction speed (1000 nm/s), constant contact time (0 ms), and constant contact force (~0.2 nN). At least 1000 force curves were used to plot adhesion force histograms for the interaction of β-peptide oligomers with hydrophobic AFM tips. Similar data were obtained in at least three independent experiments and six tip/sample combinations.

difference between the two sets of force histograms is a slight narrowing of the adhesion force distributions due to a decrease in the sample size in Figure 3E and 3F (a full discussion of the features of the force histograms that we view as significant is presented below). Overall, this result confirms that the fraction of adhesive interactions measured was sufficiently low that the force histograms in Figure 3C and 3D are dominated by single-molecule interactions. This result together with the low density of β-peptide immobilized on the surface (we calculate the maximum β-peptide density that can be covalently immobilized to the mixed monolayer containing 0.2% EG4N and 99.8% EG4 to be ~1 β-peptide oligomer per ~100 nm^2, see Supporting Information) supports our interpretation of the force histograms in Figure 3C and 3D as corresponding to single β-peptide interactions. Second, although nonrandom mixing of organothiol molecules within mixed monolayers formed on gold has been reported[51] and could lead to local clustering of β-peptides, the structural similarity of the hydroxyl- and amine-terminated thiols used in our study makes such clustering unlikely. Third, we note that the magnitudes of the adhesive forces shown in Figure 3C and 3D are in a range that is typical of single-molecule interactions.[13]

Close inspection of Figure 3C reveals that the adhesive interactions of the hydrophobic AFM tip and the **GA** oligomer give rise to a broad, asymmetric distribution of forces (0.1−0.4 nN) with a peak in frequency at 0.13 nN. The presence of this broad and asymmetric distribution of forces, with a subpopulation of strong adhesive interactions (>0.23 nN), was a general feature of the histograms measured using the **GA** sequence isomer. In contrast, we observed the adhesive interactions between the ***iso*-GA** oligomer (Figure 3D) to result in a relatively symmetric and narrow distribution of forces (0.1−0.2 nN). These differences between the force histograms for the two sequence isomers were consistently found in repeated measurements performed with independently prepared samples and different AFM tips. These results indicate that single **GA** or ***iso*-GA** β-peptides give rise to qualitatively different interaction profiles with the hydrophobic tip surface.

We hypothesized that the different features apparent in the force histograms of sequence isomers **GA** and ***iso*-GA** (Figure 3) reflect differences in the nanopatterns of cationic and hydrophobic residues projected by these 14-helical β-peptides. **GA** can present distinct faces to the hydrophobic tip because the hydrophobic ACHC and cationic β^3-hLys groups are globally segregated to opposite sides of the 14-helical conformation. In contrast, ***iso*-GA** will necessarily present a mixture of the two types of side chain to the hydrophobic tip, regardless of the orientation of the oligomer, because the cationic and hydrophobic β-amino acid residues are more uniformly distributed over the surface of the 14-helix (Figure 3C and 3D). We specifically propose that the strong adhesive interactions apparent in the force histograms for **GA** (>0.23 nN, corresponding to ~22% of adhesive interactions) result from orientations of **GA** that present the hydrophobic face, composed exclusively of ACHC residues, to the hydrophobic tip. This geometry leads to a strong hydrophobic interaction between **GA** and the tip surface, which is not possible for the ***iso*-GA** sequence isomer. Although approximately two-thirds of the surface area of the **GA** 14-helix is hydrophobic, we interpret the force histogram to indicate that only a relatively small fraction of adhesive events (~22%) result from interaction of an exclusively hydrophobic face of the β-peptide with the hydrophobic AFM tip. This interpretation of the experimental data suggests that the β-peptides are hindered in their orientational degrees of freedom at the surface. Such constraints may arise from (i) interactions between the β-peptides and the underlying self-assembled monolayer and/or (ii) constraints associated with the covalent attachment of the β-peptide to the surface. If the β-peptides possessed complete freedom to rotate, all adhesive interactions measured for **GA** would be predicted to correspond to the highly adhesive state of the system.

To test the hypothesis described above regarding the origin of the strong adhesive interactions evident in the force histogram

dx.doi.org/10.1021/ja1089183 |*J. Am. Chem. Soc.* 2011, 133, 3981–3988

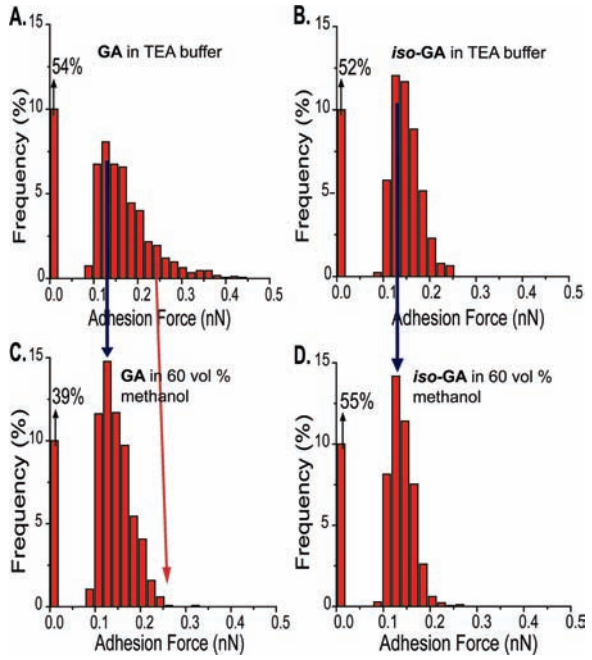

Figure 4. Force histograms of β-peptide sequence isomers and hydrophobic AFM tips in (A and B) TEA buffer, pH 7.2 and (C and D) TEA buffer containing 60 vol % methanol. The same tip/sample combination was used to obtained histograms in A and C and B and D. (A) **GA** β-peptide in TEA buffer. (B) ***iso*-GA** β-peptide in TEA buffer. (C) ***iso*-GA** β-peptide in 60 vol % methanol. (D) ***iso*-GA** β-peptide in 60 vol % methanol. Force measurements were performed at constant approach and retraction speed (1000 nm/s), constant contact time (0 ms), and constant contact force (~0.2 nN). At least 1000 force curves were used to plot adhesion force histograms for the interaction of β-peptides with hydrophobic AFM tips under both conditions. Similar data were obtained in at least three independent experiments and six tip/sample combinations.

for **GA**, we added methanol to the aqueous solution in which the force measurements were performed. Past studies have reported that addition of methanol to water (1) reduces hydrophobic interactions between proteins[52] and (2) reduces hydrophobically driven self-association of β-peptides in solution without affecting their helical secondary structure.[44] In a control study, we examined the effect of adding methanol to water (and TEA-buffered water) on the adhesion forces between two hydrophobic monolayers formed from 1-dodecanethiol (see Figure S3, Supporting Information). Our measurements indicated that adding methanol reduced the adhesive interactions between the two hydrophobic surfaces from 5.6 to 1.0 nN. Figure 4 shows the impact of addition of methanol on the force histograms characterizing the interactions of β-peptide **GA** or ***iso*-GA** with the hydrophobic AFM tip. A comparison of Figure 4A with Figure 4C reveals that the tail of the force histogram corresponding to the strong adhesive interactions of the **GA** isomer in aqueous solution was largely eliminated by addition of 60 vol % methanol, which supports our hypothesis that the subpopulation of strong adhesive interactions involving **GA** in aqueous solution is hydrophobic in origin. In contrast, as seen by comparing Figures 4B and Figure 4D, the force histogram of ***iso*-GA** was not substantially changed by addition of methanol. We note that the frequency of nonadhesive interactions in the force histograms (both in TEA- and in methanol-containing solution) is influenced by variations in the local density of immobilized β-peptide within the region of the surface probed by the AFM tip, and thus, the differences in frequencies of nonadhesive interactions seen upon addition of methanol should not be viewed as significant. We also performed force measurements in which **GA** was transferred from a 60 vol % methanol solution into aqueous TEA buffer. In these experiments, we observed the force histograms to be similar to those shown in Figure 4A and Figure 4C for the respective solvents, indicating that the effect of adding methanol was reversible. We also note that the peaks in the histograms corresponding to adhesive interactions with magnitudes of 0.1−0.2 nN were not substantially changed upon addition of methanol for either of the β-peptide oligomers. In control experiments, we measured adhesive interactions between an amine-terminated surface and a hydrophobic AFM tip in water to be unchanged by addition of methanol (similar to our observations with both β-peptide isomers in Figure 4C and 4D). This result suggests that the adhesive interactions measured between both β-peptides and hydrophobic surfaces in the presence of methanol may reflect interactions of amine groups of the β-peptides with the hydrophobic surface. The key conclusion extracted from the results in Figure 4 is that the strong adhesive forces measured between the **GA** oligomer and the hydrophobic AFM tip are due to hydrophobic interactions between the globally segregated hydrophobic ACHC groups on the surface of 14-helical **GA** and the AFM tip. This type of strong hydrophobic interaction is not possible when the ACHC groups are distributed more uniformly over the surface of the 14-helix, as is the case with ***iso*-GA**.

DISCUSSION

Our results show that sequence-dependent interactions can be measured between synthetic β-peptides and chemically modified (hydrophobic) surfaces using AFM single-molecule force spectroscopy. Previous studies have documented sequence-dependent interaction forces between biopolymers and oligo-α-peptides immobilized on surfaces. For example, the sequence-dependent affinity of α-peptides for the protein profilin has been described.[53] In addition, it has been shown that point mutations in an α-peptide sequence can change its binding affinity to DNA.[54] However, in those prior studies, because the secondary structure of the oligopeptides is not well defined, it was not possible to connect changes in the measured forces to changes in the *three-dimensional* nanopatterns of side-chain functionality presented by the α-peptides. Of particular relevance to this paper, we note that the secondary structure of oligo-α-peptides typically changes during their interaction and adsorption at interfaces (α-helix to β-sheet transitions are common).[55] Also, changes in sequence can lead to changes in α-peptide secondary structure. In contrast, because the 14-helical secondary structure of the β-peptides used in our study is stable, it is possible to attribute the different interactions of the **GA** and ***iso*-GA** isomers with the hydrophobic surface to distinct nanopatterns of functional groups presented by the 14-helical conformations of these β-peptides. The effects of methanol on the force histograms provide support for our interpretation of the force measurements in terms of variations in hydrophobic interactions that result from differences in the nanoscale presentation of ACHC groups by the two β-peptide isomers. This component of our experimental design depends upon the high conformational stability of ACHC-rich β-peptides. In contrast, addition of methanol to solutions of oligo-α-peptides or proteins will generally lead to changes in secondary structure that confound the interpretation of forces in terms of particular chemical patterns.

The conclusions extracted from the single-molecule force measurements reported in this paper are consistent with several prior studies of self-assembly of β-peptides composed of ACHC and β^3-hLys residues that fold into globally amphiphilic or nonglobally amphiphilic helices. Derivatives of **GA** have been shown to undergo hydrophobically driven self-assembly in bulk aqueous solution, but derivatives of ***iso*-GA** do not self-assemble.[41,44] Our measurements reveal the hydrophobic forces that are likely to be responsible for these differences in self-assembly behavior of β-peptide oligomers. It has been shown that methanol disrupts self-association of globally amphiphilic β-peptides.[44] Correspondingly, our results show that addition of methanol results in the elimination of the strong adhesive interactions measured for the **GA** oligomer. Molecular simulations have suggested that the association of **GA** molecules in water is driven by entropic effects arising from contacts between the hydrophobic faces of the 14-helices.[56] Our conclusion that the strong adhesive interactions observed with **GA** result from oligomer orientations that give rise to exclusively hydrophobic interactions with the AFM tip is consistent with this prior computational study.

CONCLUSIONS

Overall, the results presented here suggest that single-molecule force measurements involving β-peptide oligomers represent the basis of a promising methodology for future investigations aimed at understanding the origins of interactions that result from specific nanopatterns of chemical groups, including hydrophobic groups in water. Although the change in chemical pattern explored in this paper is relatively simple (a "globally amphiphilic" versus a "nonglobally amphiphilic" pattern), the demonstration that it is possible to measure changes in intermolecular forces that result from the change of an amphiphilic pattern in a pair of isomeric β-peptides hints that it may be possible to build upon the approach described in this paper to elucidate the impact of more subtle changes in chemical patterns on intermolecular forces. For example, a series of β-peptide oligomers with sequences that define hydrophobic domains that vary incrementally in size could enable one to quantify the influence of hydrophobic domain size on intermolecular interactions.[12] Alternatively, by placing a charged or otherwise polar residue within the hydrophobic face of a helical β-peptide oligomer, one could explore the impact of isolated polar groups on hydrophobic interactions.[12] In the long term, a more complete understanding of intermolecular forces generated by chemical nanopatterns could potentially enable the design of synthetic self-assembled materials and systems capable of executing functions that are as complex and versatile as those evident in natural systems comprised of assemblies of proteins, nucleic acids, lipids, and carbohydrates.[1]

ASSOCIATED CONTENT

Supporting Information. AFM image of a β-peptide-decorated surface, AFM force measurements between hydrophobic AFM tips and surfaces at different steps of the immobilization procedure, and AFM force measurements between monolayers formed from 1-dodecanethio1. This material is available free of charge via the Internet at http://pubs.acs.org.

AUTHOR INFORMATION

Corresponding Author
abbott@engr.wisc.edu

ACKNOWLEDGMENT

This research was supported by the University of Wisconsin—Madison Nanoscale Science and Engineering Center (NSF Grant DMR-0425880). Work in the team of Y.F.D. was supported by the National Foundation for Scientific Research (FNRS), the Foundation for Training in Industrial and Agricultural Research (FRIA), the Université Catholique de Louvain (Fonds Spéciaux de Recherche), the Federal Office for Scientific, Technical and Cultural Affairs (Interuniversity Poles of Attraction Programme), and the Research Department of the Communauté Française de Belgique (Concerted Research Action). The authors warmly thank William C. Pomerantz for assistance with the synthesis of β-peptides, Claire Verbelen for assistance with AFM force measurements, and Julie A. Last for assistance with AFM force measurements and helpful discussions.

REFERENCES

(1) Whitesides, G. M.; Mathias, J. P.; Seto, C. T. *Science* **1991**, *254*, 1312.
(2) Seeman, N. C. *Nature* **2003**, *421*, 427.
(3) Pinto, Y. Y.; Le, J. D.; Seeman, N. C.; Musier-Forsyth, K.; Taton, T. A.; Kiehl, R. A. *Nano Lett.* **2005**, *5*, 2399.
(4) Rothemund, P. W. K. *Nature* **2006**, *440*, 297.
(5) Evans, D. F.; Ninham, B. W. *J. Phys. Chem.* **1986**, *90*, 226.
(6) Israelachvili, J. N.; Mitchell, D. J.; Ninham, B. W. *J. Am. Chem. Soc., Faraday Trans. 2* **1976**, *72*, 1525.
(7) Leckband, D. E.; Israelachvili, J. N.; Schmitt, F. J.; Knoll, W. *Science* **1992**, *255*, 1419.
(8) Leckband, D. *Annu. Rev. Biophys. Biomol. Struct.* **2000**, 1.
(9) Meyer, E. E.; Rosenberg, K. J.; Israelachvili, J. N. *Proc. Natl. Acad. Sci. U.S.A.* **2006**, *103*, 15743.
(10) Huang, D. M.; Chandler, D. *Proc. Natl. Acad. Sci.* **2000**, *97*, 8324.
(11) Huang, D. M.; Geissler, P. L.; Chandler, D. *J. Phys. Chem. B.* **2001**, *105*, 6704.
(12) Chandler, D. *Nature* **2005**, *437*, 640.
(13) Hinterdorfer, P.; Dufrêne., Y. F. *Nature* **2006**, *3*, 347.
(14) Cheng, R. P.; Gellman, S. H.; DeGrado, W. F. *Chem. Rev.* **2001**, *101*, 3219.
(15) Seebach, D.; Beck, A. K.; Bierbaum, D. J. *Chem. Biodivers.* **2004**, *1*, 1111.
(16) Hecht, S.; Huc, I. *Foldamers: Structure, Properties and Applications*; Wiley-VCH: Weinheim, Germany, 2007.
(17) Zhang, L.; Wang, C.; Cui, S.; Wang, Z.; Zhang, X. *Nano Lett.* **2003**, *3*, 1119.
(18) Gumpp, H.; Puchner, E. M.; Zimmermann, J. L.; Gerland, U.; Gaub, H. E.; Blank, K. *Nano Lett.* **2003**, *3*, 3290.
(19) Valiaev, A.; Lim, D. W.; Oas, T. G.; Chilkoti, A.; Zauscher, S. *J. Am. Chem. Soc.* **2007**, *129*, 6491.
(20) Staii, C.; Wood, D. W.; Scoles, G. *Nano Lett.* **2008**, *8*, 2503.
(21) Valiaev, A.; Lim, D. W.; Schmidler, S.; Clark, R. L.; Chilkoti, A.; Zauscher, S. *J. Am. Chem. Soc.* **2008**, *130*, 10939.
(22) Stevens, M. M.; Allen, S.; Davies, M. C.; Roberts, C. J.; Sakata, J. K.; Tendler, S. J. B.; Tirrell, D. A.; Williams, P. M. *Biomacromolecules* **2005**, *6*, 1266.
(23) Gilbert, Y.; Deghorain, M.; Wang, L.; Xu, B.; Pollheimer, P. D.; Gruber, H. J.; Errington, J.; Hallet, B.; Haulot, X.; Verbelen, C.; Hols, P.; Dufrêne, Y. F. *Nano Lett.* **2007**, *7*, 796.
(24) Hinterdorfer, P.; Baumgartner, W.; Gruber, H. J.; Schilcher, K.; Schindler, H. *Proc. Natl. Acad. Sci.* **1996**, *93*, 3477.
(25) Ros, R.; Schwesinger, F.; Anselmetti, D.; Kubon, M.; Schafer, R.; Pluckthun, A.; Tiefenauer, L. *Proc. Natl. Acad. Sci.* **1998**, *95*, 7402.
(26) Berquand, A.; Xia, N.; Castner, D. G.; Clare, B. H.; Abbott, N. L.; Dupres, V.; Adriaensen, Y.; Dufrêne, Y. F. *Langmuir* **2005**, *21*, 55157.

(27) Dupres, V.; Menozzi, F. D.; Locht, C.; Clare, B. H.; Abbott, N. L.; Cuenot, S.; Bompard, C.; Raze, D.; Dufrene, Y. F. *Nat. Methods* **2005**, *2*, 515.
(28) Florin, E. L.; Moy, V. T.; Gaub, H. E. *Science* **1994**, *264*, 415.
(29) Lee, G. U.; Kidwell, D. A.; Colton, R. J. *Langmuir* **1994**, *10*, 354.
(30) Shi, Q.; Chien, Y.-H.; Leckband, D. *J. Biol. Chem.* **2008**, *283*, 28454.
(31) Lee, G. U.; Chrisey, L. A.; Colton, R. J. *Science* **1994**, *266*, 771.
(32) Ray, C.; Brown, J. R.; Akhremitchev, B. B. *J. Phys. Chem. B* **2006**, *110*, 17578.
(33) Geisler, M.; Pirzer, T.; Ackerschott, C.; Lud, S.; Garrido, J.; Scheibel, T.; Hugel, T. *Langmuir* **2008**, *24*, 1350.
(34) Pirzer, T.; Hugel, T. *ChemPhysChem* **2009**, *10*, 2795.
(35) Horinek, D.; Serr, A.; Geisler, M.; Pirzer, T.; Slotta, U.; Lud, S. Q.; Garrido, J. A.; Scheibel, T.; Hugel, T.; Netz, R. R. *Proc. Natl. Acad. Sci.* **2008**, *105*, 2842.
(36) Appella, D. H.; Christianson, L. A.; Karle, I. L.; Powell, D. R.; Gellman, S. H. *J. Am. Chem. Soc.* **1996**, *118*, 13071.
(37) DeGrado, W. F.; Cheng, R. P. *J. Am. Chem. Soc.* **2002**, *124*, 11564.
(38) Raguse, T. L.; Lai, J. R.; Gellman, S. H. *J. Am. Chem. Soc.* **2003**, *125*, 5592.
(39) Lee, M.; Raguse, T. L.; Schinner, M.; Pomeratz, W. C.; Wang, X.; Wipf, P.; Gellman, S. H. *Org. Lett.* **2007**, *9*, 1801.
(40) Vaz, E.; Pomerantz, W. C.; Geyer, M.; Gellman, S. H.; Brunsveld, L. *ChemBioChem* **2008**, *9*, 2254.
(41) Pomerantz, W. C.; Abbott, N. L.; Gellman, S. H. *J. Am. Chem. Soc.* **2006**, *128*, 8730.
(42) Pomerantz, W. C.; Yuwono, V. M.; Pizzey, C. L.; Hartgerink, J. D.; Abbott, N. L.; Gellman, S. H. *Angew. Chem., Int. Ed.* **2008**, *47*, 1241.
(43) Pizzey, C. L.; Pomerantz, W. C.; Sung, B. J.; Yuwono, V. M.; Gellman, S. H.; Hartgerink, J. D.; Yethiraj, A.; Abbott, N. L. *J. Chem. Phys.* **2008**, *129*, 095103.
(44) Pomeratz, W. C.; Grygiel, T. L. R.; Lai, J. R.; Gellman, S. H. *Org. Lett.* **2008**, *10*, 1799.
(45) Muller, M. M.; Windsor, M. A.; Pomerantz, W. C.; Gellman, S. H.; Hilvert, D. *Angew. Chem., Int. Ed.* **2009**, *48*, 922.
(46) Pomerantz, W. C.; Cadwell, K. D.; Hsu, Y. J.; Gellman, S. H.; Abbott, N. L. *Chem. Mater.* **2007**, *19*, 4436.
(47) Noy, A.; Frisbie, C. D.; Roznyai, L. F.; Wrighton, M. S.; Lieber, C. M. *J. Am. Chem. Soc.* **1995**, *117*, 7943.
(48) A. Noy, A.; Vezenov, D. V.; Lieber, C. M. *Annu. Rev. Mater. Sci.* **1997**, *27*, 381.
(49) Clare, B. H.; Abbott, N. L. *Langmuir* **2005**, *21*, 6451.
(50) Bai, Y.; Liu, X.; Cook, P.; Abbott, N. L.; Himpsel, F. J. *Langmuir* **2010**, *26*, 6464.
(51) Ballav, N.; Terfort, A.; Zharnikov, M. *J. Phys. Chem. C* **2009**, *113*, 3697.
(52) Kamatari, Y. O.; Konno, T.; Kataoka, M.; Akasaka, K. J. *J. Mol. Biol.* **1996**, *259*, 512.
(53) Okada, T.; Sano, M.; Yamamoto, Y.; Muramatsu, H. *Langmuir* **2008**, *24*, 4050.
(54) Eckel, R.; Wilking, S. D.; Becker, A.; Sewald, N.; Ros, R.; D. A *Angew. Chem., Int. Ed.* **2005**, *44*, 3921.
(55) Sethuraman, A.; Vedantham, G.; Imoto, T.; Przybycien, T.; Belfort, G. *Proteins* **2004**, *56*, 669.
(56) Miller, C. A.; Gellman, S. H.; Abbott, N. L.; Pablo, J. J. d. *Biophys. J.* **2009**, *96*, 4349.